S. A. Kozyukhin[1], M. Krbal[2], S. Kohara[3], A. A. Kononov[4, *], A. V. Kolobov[4]

As_2S_3 glass quenched under a weak magnetic field

[1] N.S. Kurnakov Institute of General and Inorganic Chemistry of the Russian Academy of Sciences, Laboratory of Chemistry of Coordinating Polynuclear Compounds, Moscow, Russia

[2] University of Pardubice, Center of Materials and Nanotechnologies, Faculty of Chemical Technology, Pardubice, Czech Republic

[3] National Institute for Materials Science, Research Center for Advanced Measurement and Characterization, Tsukuba, Japan

[4] Herzen State Pedagogical University of Russia, Department of Physical Electronics, St. Petersburg, Russia

E-mail: kononov_aa@icloud.com (A. A. Kononov)

S. A. Kozyukhin ORCID: 0000-0002-7405-551X

M. Krbal ORCID: 0000-0002-8317-924X

S. Kohara ORCID: 0000-0001-9596-2680

A. A. Kononov ORCID: 0000-0002-5553-3782

A. V. Kolobov ORCID: 0000-0002-8125-1172

Abstract

S- and Se-based chalcogenide glasses are intrinsically metastable and exhibit a number of photo-induced effects unique to this class of materials, reversible photostructural changes being a major example. Such changes manifest themselves as reversible darkening under the exposure to band gap light and are usually interpreted in terms of the formation of valence alternation pairs and 'wrong' bonds. Some time ago it was shown that quenching the As_2S_3 melt under a weak magnetic field also results in a decrease of the glass optical band gap. In this work, we report the results of comparative Extended X-ray absorption fine structure (EXAFS) and high-energy X-ray diffraction studies of the local structure of the As_2S_3 glass formed through quenching the melt under a weak magnetic field and without it. Based on these experiments and density functional theory simulations, we propose a model of the structural nanoscale modification of diamagnetic As_2S_3 under a magnetic field.

Keywords: chalcogenide glasses, As_2S_3, magnetic field, local structure

Declarations

Funding

This work has been partially supported by a joint Russian-Czech project funded by the Russian Foundation for Basic Research (grant 19-53-26017) and the Czech Science Foundation (grant 20-23392J).

Acknowledgments

The authors are grateful to Paul Fons for his help in generating the in-silico amorphous As_2S_3 structure. Synchrotron experiments were performed at Spring-8 (Japan): EXAFS measurements - at beam line BL01B1, high-energy X-ray diffraction measurements - at beam line BL04B2 (2014B1242 proposal),. The authors are also grateful to E.A. Chechetkina for insightful discussions.

Conflicts of interest/Competing interests (include appropriate disclosures)

The authors declare that they have no conflicts of interest.

Availability of data and material (data transparency)

The data that support the findings of this study are available from the corresponding author upon reasonable request.

Code availability (software application or custom code)

N/A

Relevance Summary

The present work reports on EXAFS and high-energy X-ray diffraction studies of the nanometer scale local structure of the As_2S_3 glass formed under a weak magnetic field and without it. As_2S_3 is of great topical interest as a material with a number of photo-indued phenomena (reversible photostructural change being a most characteristic example). Based on the above experiments and density functional theory simulations, we propose a model of the structural modification of As_2S_3 under a magnetic field.

1 Introduction

Chalcogenide glasses, of which As_2S_3 is a typical representative, exhibit a number of photo-indued phenomena, reversible photostructural change being a most characteristic example (for reviews see [1, 2]). Reversible photo-structural change, experimentally detected by structure-sensitive techniques such as Raman scattering [3], x-ray scattering [4] and extended x-ray absorption fine structure ((EXAFS) [5, 6] manifests itself as photodarkening [7], when the optical band gap decreases upon illumination. The initial properties can be restored by subsequent annealing at temperatures close to the glass-transition temperature. The band gap decrease depends on the material composition and can reach a value as large as 0.3 eV [8], which is close to 15% of the initial gap value. The photodarkening is usually accompanied by volume expansion [9, 10]. On the nanometer scale, photodarkening has been explained by bond switching [11], the formation of photo-induced valence alternation pairs [5] and the formation of 'wrong' bonds [3]. It was also proposed that so-called soft modes may serve to generate states with negative correlation energy responsible for photodarkening [12]. Computer studies also concluded that interchain interaction was enhanced in selenium as evidenced by the formation of dynamic covalent bonds between neighboring chains [13].

Interestingly, darkening has also been reported for the As_2S_3 glass quenched under a weak magnetic field [14], the result being very intriguing because the material does not contain magnetic elements. In this paper, we report the results of comparative EXAFS and high-energy x-ray diffraction studies of As_2S_3 formed through quenching the melt under a weak magnetic field and in its absence. Based on the experimental results and density functional simulations we propose a plausible nanoscale model of the effect of magnetic field on the structure of diamagnetic As_2S_3 glass.

2. Experiments and simulations

As_2S_3 compositions were prepared in evacuated (10^{-4} Pa) and sealed fused quartz ampoules from elemental ingredients with purity no worse than four nines preliminary purified by distillation. The synthesis procedure lasted near 14 h was portioned in a few step-wise stages with fixed temperatures kept during 2 h and further vibrational mixing. The maximum temperature of synthesis was 720 K. The ingots were then air-quenched to a glassy state, which was controlled visually by a characteristic conchoidal fracture. Then the glass samples in evacuated quartz ampoules were heated in a furnace located in air gap in a solenoid. The processing mode was as follows: heating to 670 K, holding for 30 min. and then cooling to room temperature with the furnace turned off.

One glass sample was used as a control and, accordingly, was not exposed to the magnetic field, and the other was exposed to the magnetic field of a solenoid (H = 250 Oe) during the exposure at 670 K and subsequent cooling.

Extended X-ray absorption fine structure (EXAFS) measurements were performed in transmission mode at beam line BL01B1 at Spring-8. Samples were powders of As_2S_3 glass quenched with and without a magnetic field [14]. They were mixed with BN to achieve an absorption edge jump of unity. Analysis of the experimental data was performed using the Athena/Arthemis packages [15].

The high-energy X-ray diffraction experiment was performed at beamline BL04B2 at the SPring-8 synchrotron radiation facility, using a two-axis diffractometer dedicated to the study of disordered materials [16]. The energy of the incident X-rays was 112.8 keV. The raw data were corrected for polarization, absorption, the background, and the contribution of Compton scattering was subtracted using standard data analysis software. The fully corrected data were normalized to give a Faber-Ziman [17] total structure factor. The total correlation function *T(R)* was derived by the Fourier transform of *S(Q)*.

Molecular dynamics calculations of As_2S_3 were carried out using the plane wave pseudopotential code VASP 5.4.4 using a NVT ensemble [18]. A total of 240 atoms were included in the simulation cell with a density 3.49 g/cm^3. The Gamma point with a Gaussian smearing of 0.05 eV was used for Brillouin zone integration. A value of 260 eV was used for the plane wave cutoff as recommended by the VASP developers. The Perdew-Burke-Ernzerhof exchange correlation functional was utilized [19]. The projected-augmented method in which the outermost *s*-and *p*-electrons were treated as valence electrons was used to correct for the effect of the core electrons within the augmentation sphere [20]. The amorphous phase was generated by the following procedure. The initial structure was randomized by heating the structure to 3000 K followed by cooling to a temperature just above the melting point 900 K over a period of 45 ps. The amorphous phase was generated by quenching from 900 to 300 K over a duration of 15 ps.

The electronic structure of the orpiment and tetradymite crystalline phases of As_2S_3 were simulated using the plane-wave code CASTEP [21]. The PBE functional [19] was used to optimise the structures.

3 Results and discussion

A change in optical absorption in chalcogenide glasses that manifests itself as photodarkening is usually associated with photostructural change. In many cases darkening is observed under exposure of chalcogenide glasses to band gap light but it can also be induced by other agents. In particular, it has been reported that bulk ingots of As_2S_3 glasses quenched under a weak magnetic field and without the magnetic field [14] look quite different (figure 1). The visual difference is twofold. Firstly, the glass quenched under a magnetic field is notably darker, secondly, it breaks in a different manner. Both results demonstrate the structure, i.e. the bonding, difference in the two cases.

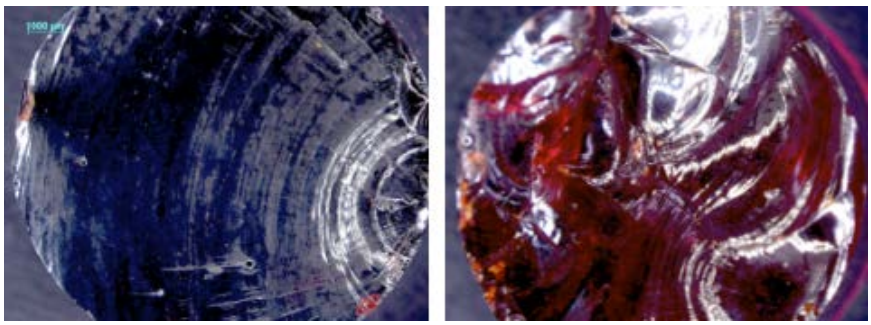

Fig. 1 Bulk As_2S_3 glass quenched under a weak magnetic field (left) and without a magnetic field (right)

To investigate the structural differences between these two structures on the nanometer scale, we performed X-ray absorption and high-energy X-ray diffraction measurements. Figures 2 and 3 show raw EXAFS oscillations and the corresponding Fourier transforms of the two samples alongside with the fitting results. One can see that in the

sample annealed under magnetic field the amplitude of the oscillations at higher *k* is slightly larger. The difference is also visible in the Fourier transformed spectra. Another aspect that can be noticed is a higher white line intensity in the sample quenched without the magnetic field.

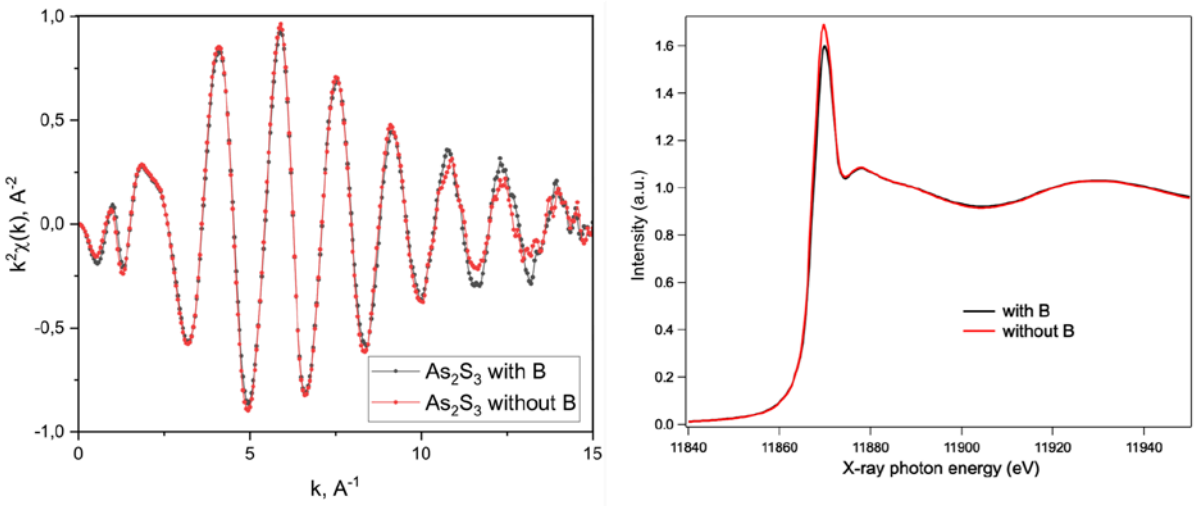

Fig. 2 Raw EXAFS oscillations (left) and XANES spectra (right) of As_2S_3 quenched without (red) and under (black) weak magnetic field

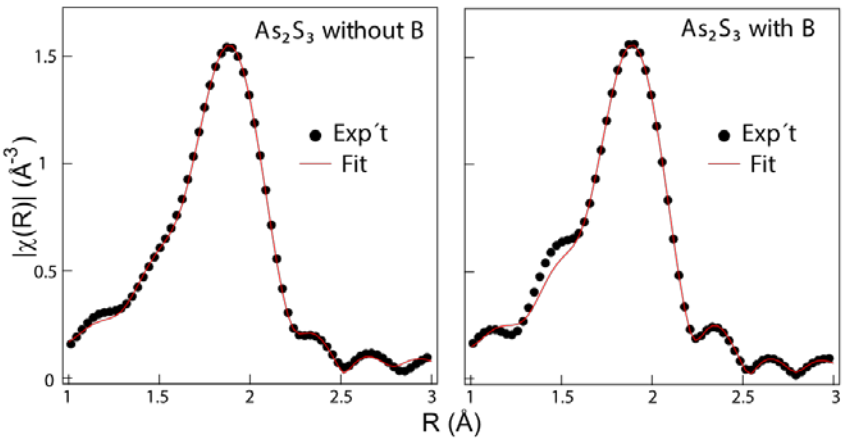

Fig. 3 Fourier transformed spectra of As_2S_3 quenched without (left) and under (right) weak magnetic field (dots). The fitting results are also shown (solid lines)

The fitting of the experimental data (Table 1) yielded the average As-S bond length of 2.27±0.02 Å, while the As-S partial coordination number was 2.7 in the sample quenched without field and 2.3 in the sample with field. At the same time, the As-As partial coordination number was higher (2.8 vs. 0.8) in the sample quenched with field. It should be noted, however, that the uncertainties (Table 1) for the As-As coordination numbers were rather large. The larger concentration of As-As bonds in the sample annealed with field is not unreasonable since photodarkening was also found to correlate with an increased concentration of As-As bonds [3].

Table 1. EXAFS fitting results (partial coordination numbers - *N*, and bond lengths - *R*) for As_2S_3 quenched without and with a weak magnetic field

Structural parameter	without field	with field
N_{As-S}	2.71 ± 0.14	2.30 ± 0.11
R_{As-S}, Å	2.27 ± 0.01	2.27 ± 0.01
N_{As-As}	0.78 ± 0.58	2.79 ± 1.88
R_{As-As}, Å	2.53± 0.02	2.53± 0.02

As an alternative approach, the data sets were fitted assuming the presence of shorter and longer bonds in the linear fragments by analogy with shorter and longer bonds in amorphous GeTe. In this scenario, the fitting quality was comparable to the previous case.

We further measured high-energy X-ray diffraction. Figure 4 shows the structure factors *S(Q)* and total correlation functions *T(R)* of As_2S_3 quenched without (blue) and under (red) weak magnetic field. Again, despite the high quality of the experimental data, the differences between the two structures are too small to draw any definitive conclusions. One can speculate that the difference is due to the presence of a rather small concentration of specific structural defects (such as valence alternation pairs of linear fragments) that are not detectable by the techniques used.

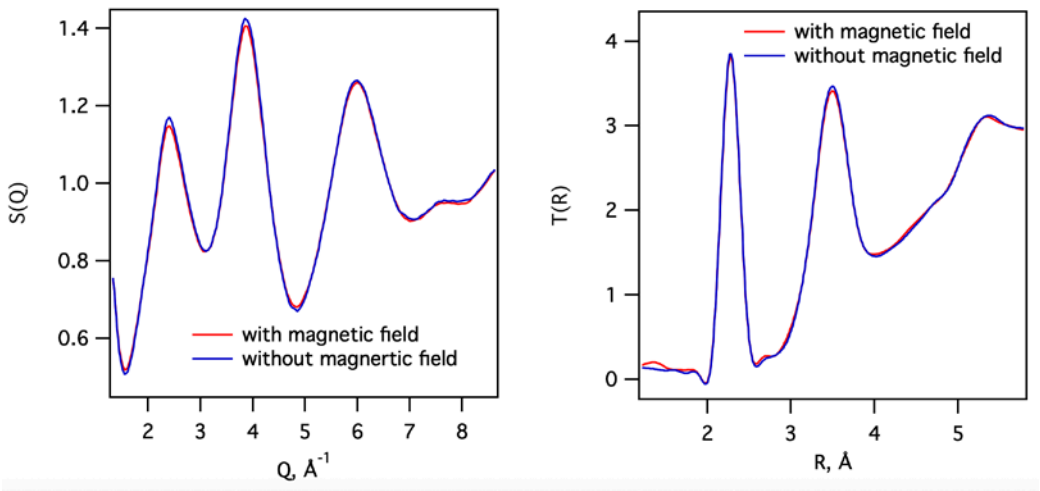

Fig. 4 Structure factors *S(Q)* and total correlation functions *T(R)* of As_2S_3 quenched without (blue) and under (red) weak magnetic field

To obtain further insights into the structural differences we also performed density functional theory (DFT) simulations. Because the local structure of an amorphous material is generally similar to that of the corresponding crystal [22], we first consider possible crystalline structures. Crystalline As_2S_3 possess the orpiment structure, however its heavier isoelectronic homologues Sb_2Te_3, Bi_2Se_3, and Bi_2Te_3 crystallise into a layered tetradymite structure (insets to figure 5). While the bonding geometry in the former satisfies the 8-*N* rule [23] typically observed in glasses

(chalcogen atoms are two-fold coordinated and pnictogens are three-fold coordinated), in the latter the 8-*N* rule is violated.

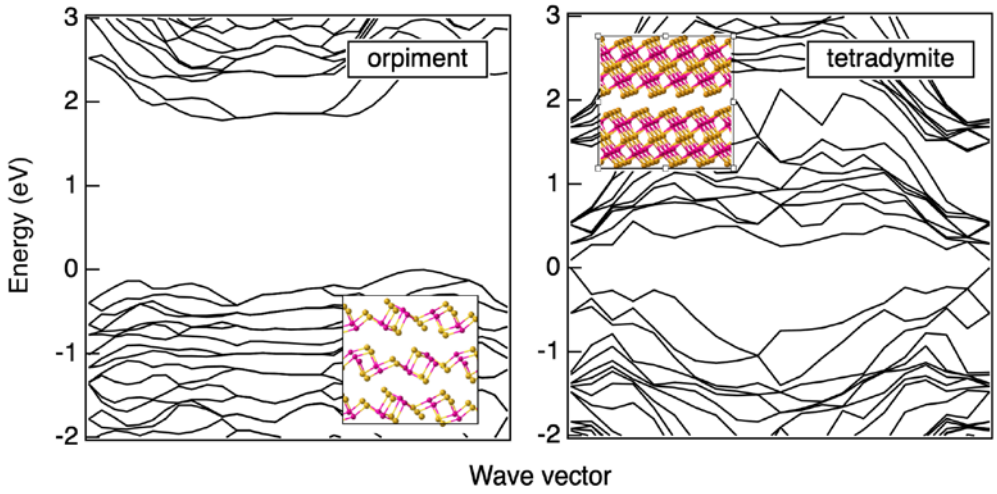

Fig. 5 Band diagrams of the orpiment (left) and tetradymite (right) structures of As_2S_3 obtained through DFT simulations. The insets show the two different structures. Since the purpose of the figure is to demonstrate the large difference in the band gap values and not to discuss the electronic structure itself, the *k*-points are not indicated

It is not unnatural to assume that in a glass fragment reminiscent of both structures can be present. Indeed, in *in-silico* generated amorphous As_2S_3 (figure 6) both the fragments characteristic of the orpiment phase, and linear atomic fragments reminiscent of the tetradymite phase are formed. We note in passing that extended linear fragments were also found in amorphous of Sb_2Te_3 [24]. It should also be noted that such extended fragments, called hypervalent bonds, were introduced by Dembovsky and Chechetkina [25] as major defects in chalcogenide glasses. Furthermore, the idea of the formation of tetradymite-like structural fragments with shorter and longer bonds was initially proposed by Dembovsky and Chechetkina as self-organization of hypervalent bonds, or bond waves [26].

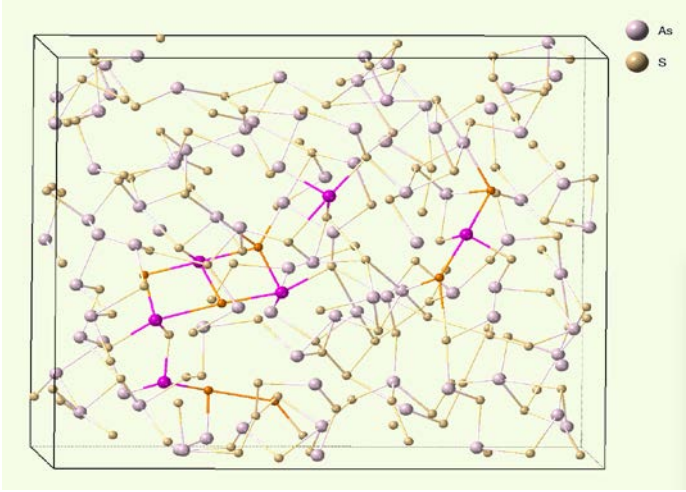

Fig. 6 *In-silico* melt-quenched amorphous As_2S_3. In addition to fragments satisfying the 8-*N* rule, linear fragments marked by brighter colors and As-S-As-S squares are clearly visible

Comparison of the band structures of the orpiment and tetradymite phases shown in figure 5 demonstrates that the tetradymite structure with QLs has a significantly smaller band gap (0.1 eV vs. 2.1 eV). Consequently, if an external magnetic field promotes the formation of linear fragments, a larger concentration of the tetradymite phase should result in a darker glass. It is still not clear how and why the magnetic field effects the formation of linear tetradymite fragments but it is interesting to notice that rather strong effects of an external magnetic field were also reported for interfacial phase-change materials containing layers of the tetradymite Sb_2Te_3 phase [27]. Effects of weak magnetic field on other diamagnetic materials are reviewed in [28].

The linear fragments are formed through the involvement of lone-pair electrons interacting with back-lobes of covalently bonded p-orbitals [25]. Recently, the important role of lone-pair electrons in the formation of multicenter bonds has been stressed in various publications [29, 30] underscoring their significance for chalcogenide-based materials. One can assume that controlling the concentration of lone-pair electrons, e.g. through doping with transition metals can serve to modify the ability of As_2S_3-like chalcogenide glasses to form linear fragments, which, as noted above, was argued to be one of the reasons of good glass-forming ability of chalcogenide glasses. Consequently, the glass forming ability should change as well as, possibly, also the magnitude of photo-induced anisotropy in such glasses.

4 Conclusion

In conclusion, based on the results of experimental EXAFS and high-energy x-ray diffraction studies combined with density functional simulations, we propose that the presence of an external weak magnetic field may affect the ability of glassy As_2S_3 to form linear fragments with multicenter bonds combined with a higher concentration of As-As bonds. At the same time, we notice that the experimentally measured difference between the two sets of samples is rather small and consequently this conclusion is speculative. Further studies of the nanoscale structure are needed to understand the unusual effect of a weak magnetic field on the diamagnetic As_2S_3 glass.

References

1. A.V. Kolobov, *Photo-induced Metastability in Amorphous Semiconductors* (John Wiley & Sons, Berlin, 2006).
2. K. Tanaka, K. Shimakawa, *Amorphous Chalcogenide Semiconductors and Related Vaterials* (Springer, London, 2011). https://doi.org/10.1007/978-1-4419-9510-0
3. M. Frumar, A.P. Firth, A.E. Owen, Philos. Mag. B **50**, 463 (1984). https://doi.org/10.1080/13642818408238871
4. K. Tanaka, Appl. Phys. Lett. **26**, 243 (1975). https://doi.org/10.1063/1.88136
5. A.V. Kolobov, H. Oyanagi, K. Tanaka, K. Tanaka, Phys. Rev. B **55**, 726 (1997). https://doi.org/10.1103/PhysRevB.55.726
6. G. Chen, H. Jain, S. Khalid, J. Li, D.A. Drabold, S.R. Elliott, Solid State Commun. **120**, 149 (2001). https://doi.org/10.1016/S0038-1098(01)00354-4
7. J.S. Berkes, S.W. Ing, W.J. Hillegas, J. Appl. Phys. **42**, 4908 (1971). https://doi.org/10.1063/1.1659873
8. S.B. Gurevich, N.N. Ilyashenko, B.T. Kolomiets, V.M. Lyubin, V.P. Shilo, Phys. Stat. Sol. A **26**, K127 (1974). https://doi.org/10.1002/pssa.2210260251
9. K. Tanaka, Phys. Rev. B **57**, 5163 (1998). https://doi.org/10.1103/PhysRevB.57.5163
10. H. Hisakuni, K. Tanaka, Appl. Phys. Lett. **65**, 2925 (1994). https://doi.org/10.1063/1.112533
11. S.R. Elliott, J. Non-Cryst. Solids **81**, 71 (1986). https://doi.org/10.1016/0022-3093(86)90260-7

12. M.I. Klinger, S.N. Taraskin, Phys. Rev. B **52**, 2557 (1995). https://doi.org/10.1103/PhysRevB.52.2557
13. J. Li, D.A. Drabold, Phys. Rev. Lett. **85**, 2785 (2000). https://doi.org/10.1103/PhysRevLett.85.2785
14. E.A. Dembovsky, S.A. Chechetkina, S.A. Kozyukhin, Pis'ma v ZhETF **41**, 74 (1984) (in Russian)
15. B. Ravel, M. Newville, J. Synch. Rad. **12**, 537 (2005). https://doi.org/10.1107/S0909049505012719
16. K. Ohara, Y. Onodera, M. Murakami, S. Kohara, J. Physics: Cond. Matter **33**, 383001 (2021). https://doi.org/10.1088/1361-648X/ac0193
17. T. Faber, J. Ziman, Philos. Mag. **11**, 153 (1965). https://doi.org/10.1080/14786436508211931
18. G. Kresse, J. Hafner, Phys. Rev. B **49**, 14251 (1994). https://doi.org/10.1103/PhysRevB.49.14251
19. J. Perdew, K. Burke, M. Ernzerhof, Phys. Rev. Lett. **77**, 3865 (1996). https://doi.org/10.1103/PhysRevLett.77.3865
20. G. Kresse, D. Joubert, Phys. Rev. B **59**, 1758 (1999). https://doi.org/10.1103/PhysRevB.59.1758
21. S.J. Clark, S, M.D. Segall, C.J. Pickard, P.J. Hasnip, M.J. Probert, K. Refson, M.C. Payne, Z. Kristallographie, **220**, 567 (2005). https://doi.org/10.1524/zkri.220.5.567.65075
22. R. Zallen, *The Physics of Amorphous Solids* (Wiley, New York, 1983).
23. N.F. Mott, Adv. Phys. **16**, 49 (1967). https://doi.org/10.1080/00018736700101265
24. T.H. Lee, S.R. Elliott, Phys. Stat. Sol. - RRL **15**, 2000516 (2021). https://doi.org/10.1002/pssr.202000516
25. S.A. Dembovsky, E.A. Chechetkina, *Glass Formation* (Nauka, Moscow, 1990) (in Russian)
26. S.A. Dembovsky, E.A. Chechetkina, in Photo-Induced Metastab. Amorphous Semicond., ed. by A.V. Kolobov (Wiley-VCH, Weinheim, 2003), p. 299.
27. J. Tominaga, Y. Saito, K. Mitrofanov, N. Inoue, P. Fons, A.V. Kolobov, H. Nakamura, N. Miyata, Adv. Func. Mater. **27**, 1702243 (2017). https://doi.org/10.1002/adfm.201702243
28. Yu.I. Golovin, Phys. Solid State **46**, 789 (2004). https://doi.org/10.1134/1.1744954
29. E.J. Skoug, D.T. Morelli, Phys. Rev. Lett. **107**, 235901 (2011). https://doi.org/10.1103/PhysRevLett.107.235901
30. A.V. Kolobov, P. Fons, J. Tominaga, S.R. Ovshinsky, Phys. Rev. B **87**, 165206 (2013). https://doi.org/10.1103/PhysRevB.87.165206